

# Spectrum of Blunt Chest Injuries

*Nisa Thoongsuwan, MD, Jeffrey P. Kanne, MD, and Eric J. Stern, MD*

**Key Words:** Contusion, laceration, pneumothorax

*(J Thorac Imaging 2005;20:89–97)*

## IMAGING FOR BLUNT CHEST TRAUMA

The chest radiograph remains the initial study for assessing patients sustaining blunt trauma to the chest, and many common injuries can be identified by the chest radiograph alone. However, in severely injured patients, the ideal upright, full inspiratory PA chest radiograph cannot be obtained. Portable supine radiographs, often suffering from poor positioning, poor inspiration, or artifact from an underlying backboard or overlying monitoring equipment, are generally the rule rather than the exception, and many injuries may be difficult to detect on these suboptimal studies.

It is essential to identify on the chest radiograph life threatening conditions such as pneumothorax, hemothorax, abnormal mediastinum (possibly indicating aortic or other great vessel injury), and thoracic spine fracture, as well as malpositioned life support devices. The technical limitations of a chest radiograph should be declared when it is difficult or impossible to exclude a life-threatening injury, and alternative imaging studies should be suggested.<sup>1</sup>

CT of the chest, particularly with the development multidetector-row CT (MDCT) scanners, has become a common examination for imaging the trauma patient with known or suspected thoracic injury, as CT scanners are available in almost all trauma centers. The fast scanning time of MDCT allows for single-breath-hold scanning, fewer motion artifacts, and improved contrast bolus imaging. Additionally, thinner collimation provides isotropic voxels, allowing for multiplanar reformations while maintaining spatial resolution.

Magnetic resonance imaging (MRI) has many advantages for imaging the chest, including no need for iodinated contrast material, lack of ionizing radiation, and multiplanar imaging capabilities. However, scan times can be lengthy, and monitoring critically ill patients can be difficult, limiting the role of MRI for evaluating trauma patients.

This pictorial essay will review the spectrum of injuries that occur in the chest following blunt trauma, focusing on the radiographic and CT findings.

## LUNG PARENCHYMA

### Pulmonary Contusion

Pulmonary contusion is the traumatic extravasation of blood into the lung parenchyma without significant laceration and is the most common pulmonary injury resulting from blunt chest trauma.<sup>2</sup>

The radiographic findings of pulmonary contusion (Fig. 1) are non-specific, ranging from irregular confluent or discrete nodular opacities to large opacities in a non-anatomical distribution, and are dependent on the site of injury.<sup>3</sup> The time course of the development and evolution of parenchymal opacity is a key to identifying this injury, as pulmonary contusion typically appears within hours of injury. Uncomplicated pulmonary contusion begins to resolve on the chest radiograph after 48 to 72 hours. Complete resolution usually occurs by 10 to 14 days.<sup>4</sup>

CT is highly sensitive and is more specific than the chest radiograph for identifying pulmonary contusion.<sup>5</sup> Pulmonary contusion appears as an ill-defined area of peripheral consolidation on CT. Although chest radiographs are useful, pulmonary contusion may be obscured earlier on by other thoracic injuries or complications,<sup>6</sup> such as pleural fluid collection or lobar collapse.

### Pulmonary Laceration

Pulmonary laceration is a tear of the lung parenchyma. As a result of the recoil properties of the adjacent lung, the initial linear parenchymal tear rapidly becomes an ovoid or round space.<sup>2,7</sup> When the laceration fills with blood, it is sometimes referred to as a hematoma, and if the space fills with air, it may be called a traumatic pneumatocele. However, frequently both blood and air accumulate in these tears, and we prefer to use the more general term, laceration.

The typical radiographic appearance of pulmonary laceration is a round air or air and fluid containing lesion. They are commonly seen as isolated lesions but may be multiple. Most pulmonary lacerations are 2–5 cm in diameter but can occasionally be extremely large, exceeding 14 cm in diameter.<sup>8</sup> Pulmonary lacerations occur at the time of injury but may be obscured on the chest radiograph by surrounding pulmonary contusion, hemothorax, or pneumothorax.<sup>2,8</sup> The visibility of the lesion also depends on the size of the lesion, as well. Resolution generally takes several weeks to a month, and sometimes lacerations heal with residual scarring.

From the Department of Radiology, Harborview Medical Center, 325 9th Ave, Box 359728, Seattle, WA 98104-2499.

Reprints: Nisa Thoongsuwan, M.D., Department of Radiology, Harborview Medical Center, 325 9th Ave, Box 359728, Seattle, WA 98104-2499 (e-mail: nisa@u.washington.edu).

Copyright © 2005 by Lippincott Williams & Wilkins

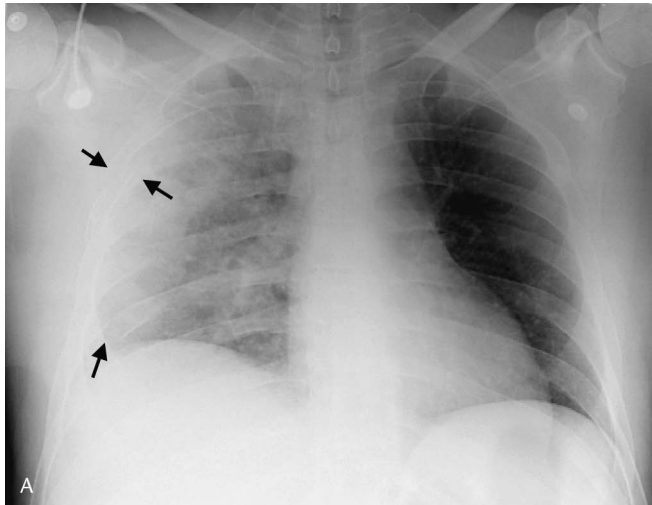


**FIGURE 1.** A, Supine chest radiograph of a 40-year-old man who fell approximately 30 feet onto concrete shows peripheral pulmonary opacity over the right hemithorax adjacent to a ribs fracture (arrows). CT scan of the chest on the same day (B, C) shows opacity (asterisks) adjacent to the fractured rib (arrow), consistent with pulmonary contusion. The right pneumothorax (asterisk) is not seen on supine chest radiograph.

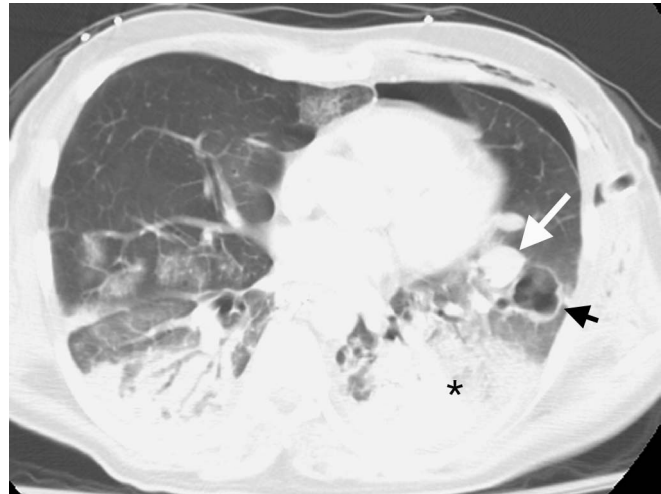


**FIGURE 2.** CT of the chest of a 47-year-old man who fell approximately 20 feet from a ladder shows type 1 pulmonary lacerations; one lesion contains blood (white arrow) and the other contains air (black arrow). Left pneumothorax and surrounding pulmonary contusion (black asterisk) are also present.

Pulmonary lacerations can be categorized into 4 types based on the mechanism of injury, as described by Wagner et al.<sup>7</sup>

**Type 1** pulmonary laceration (Fig. 2) results from sudden compression of the pliable chest wall against the closed glottis, wherein the air-containing parenchyma ruptures. These are typically large (2–8 cm.) and are located deep within the pulmonary parenchyma.

**Type 2** pulmonary laceration (Fig. 3) occurs from shearing forces as the lung is squeezed over the vertebral bodies from rapid compression of the chest wall. This type of



**FIGURE 3.** CT of the chest of an 18-year-old man who was hit by a car while on a motorcycle shows an elliptical-shaped type 2 pulmonary laceration (arrow) in the left paravertebral region.

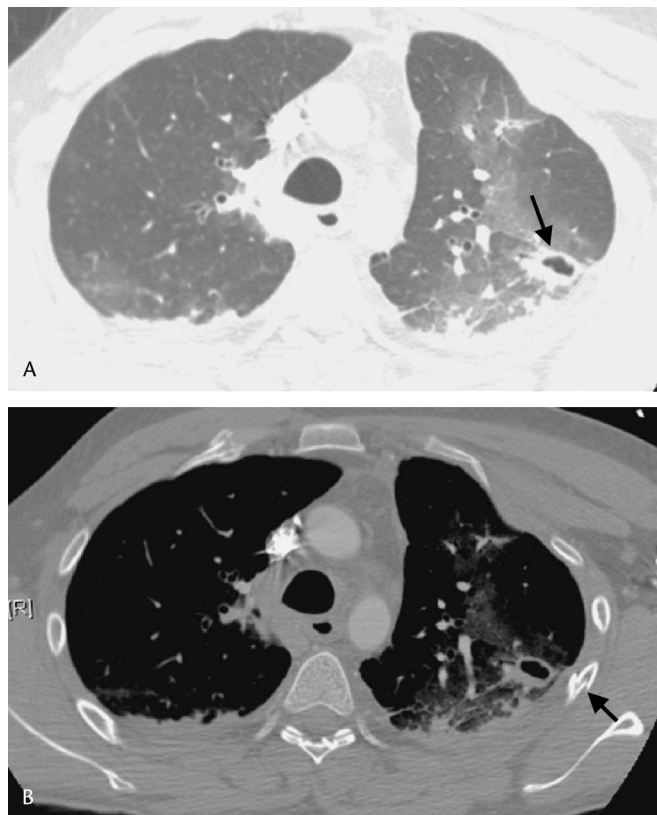


**FIGURE 4.** A, CT of the chest of a 32-year-old man who fell 35 feet shows a type 3 pulmonary laceration at the left lung periphery (arrow). B, The adjacent rib fracture is better seen with bone window settings (arrow).

laceration typically occurs in the paraspinal lung parenchyma and may have an elongated rather than spherical appearance.

**Type 3** pulmonary laceration (Fig. 4) is a penetrating injury caused by puncture from a fractured rib fragment and typically appears as a small peripheral lucency intimately associated with an adjacent rib fracture. These types of injuries are often multiple.

**Type 4** pulmonary laceration is the result of a previously formed, firm pleuropulmonary adhesion causing the lung to tear when the overlying chest wall is violently compressed inward or is fractured. This type is almost always identified only at surgery or autopsy.

## PLEURA

### Pneumothorax

Pneumothorax is a leakage of gas from the air spaces of the lung parenchyma or tracheobronchial tree into the pleural space and occurs in 15–38% of patients suffering from blunt chest trauma.<sup>9,10</sup> As pneumothorax is usually associated with rib fracture, the mechanism of injury is generally a direct puncture of the visceral pleura.<sup>11</sup>

With the patient upright, pneumothorax typically appears as a crescent-shape radiolucent area, outlined medially by the sharp white line of the visceral pleura in the upper hemithorax. However, in the supine patient, gas preferentially

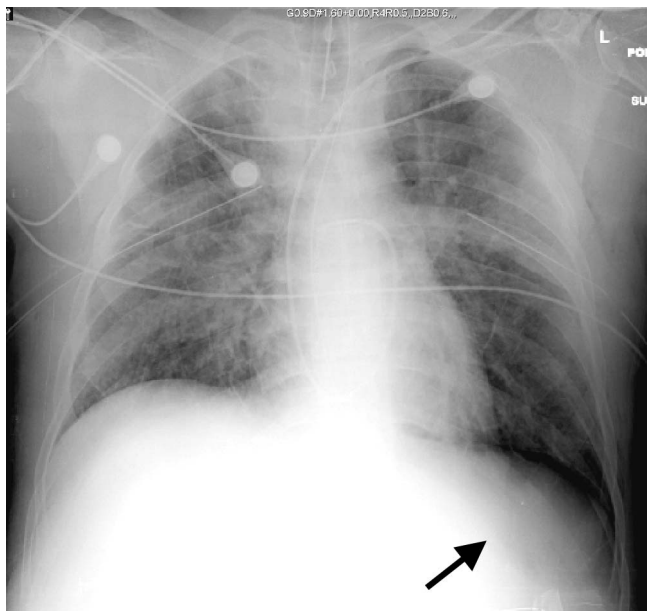


**FIGURE 5.** Supine chest radiograph of a 35-year-old man struck by a car shows a radiolucent area over the left hemidiaphragm (arrow), also called the deep sulcus sign, which represents pneumothorax on the supine radiograph. In this case, despite the chest tube, the bilateral perihilar opacity likely reflects mild edema. The side port of the left pleural drain is outside the pleural space.

collects in the antigravity-dependent portion of the pleural space, anteromedially and inferiorly. Consequently, the radiographic findings of pneumothorax in most trauma patients are different from those seen on upright radiographs. The radiographic features of pneumothorax on the supine radiograph include the deep sulcus sign (prominence of the costophrenic sulcus) (Fig. 5), basilar hyperlucency, unusual sharp delineation of the mediastinal or cardiac contour, and clear visualization of the apical pericardial fat pad.<sup>1,12,13</sup>

CT is the most accurate method for detecting pneumothorax.<sup>14</sup> Since the smallest pneumothorax can develop into a life threatening tension pneumothorax, chest CT should be considered in patients with no evidence of pneumothorax on the supine radiograph but who are at risk for pneumothorax and who will receive positive pressure ventilation.<sup>1,2,13</sup>

Tension pneumothorax is one of the most common life-threatening intrathoracic injuries caused by blunt trauma.<sup>15</sup> The diagnosis in most cases is made from clinical signs and symptoms. Radiographic findings suggestive of tension pneumothorax include increased lucency of the affected hemithorax with contralateral displacement of the mediastinum and trachea and flattening or even inversion of the ipsilateral hemidiaphragm.<sup>11</sup>

### Hemothorax

Hemothorax is the collection of blood within the pleural space. Bleeding from low pressure vessels may subside spontaneously or following pleural drain placement.<sup>1</sup> However, massive hemothorax is a life threatening condition because of potential mass effect on the heart and great vessels from the

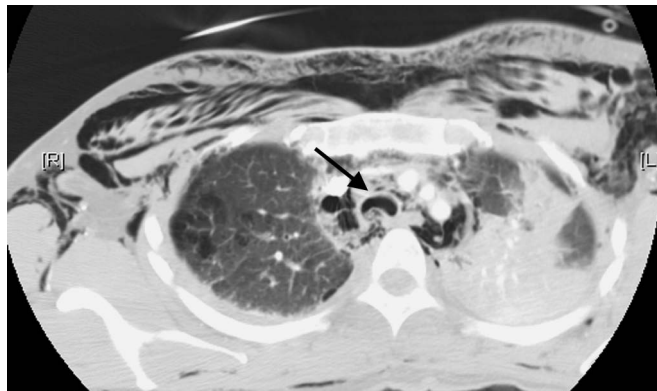


**FIGURE 6.** CT of the chest of a 34-year-old woman who was an unrestrained passenger in a high-speed motor vehicle crash shows marked pneumomediastinum and subcutaneous emphysema with the deformity of the trachea (arrow). Tracheal laceration was confirmed at bronchoscopy.

accumulated blood, acute hypovolemic shock, and hypoxia from lung collapse.<sup>16</sup>

The findings of hemothorax on the supine chest radiograph are often indirect and include diffusely increased opacity over the affected hemithorax, a homogenous crescent-shaped opacity interposed between the inner margin of the ribs and the lung, or an apical cap (a crescent-shaped opacity over the lung apices on the supine radiograph).<sup>1</sup>

On CT, particularly in the acute setting, blood products in the pleural space may have high attenuation; and when active bleeding is present, layering of different attenuation fluids may occur.

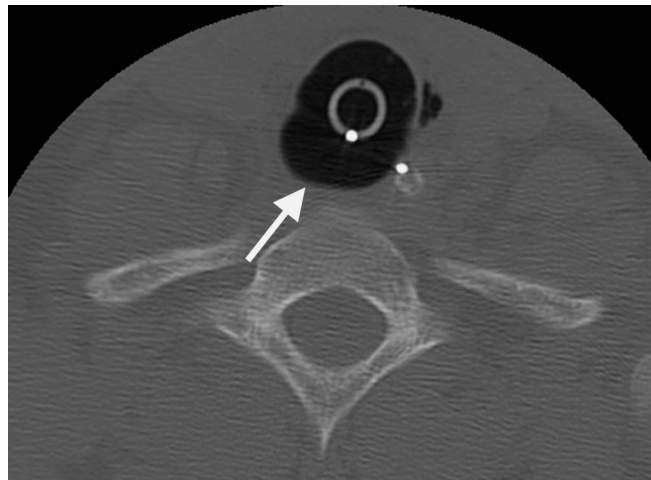


**FIGURE 7.** Image from a CT of the cervical spine of a 23-year-old woman injured in a motorcycle crash shows a bulging of the endotracheal tube balloon cuff (arrow), suggestive of tracheal injury. A disruption of the posterior membranous wall of the trachea 4 cm above the carina was confirmed at bronchoscopy.

## AIRWAY

### Tracheobronchial Laceration

Tracheal rupture from blunt chest injury accounts for approximately 15–27% of all tracheobronchial lacerations and is associated with higher overall morbidity and mortality.<sup>17–19</sup> The diagnosis of tracheal rupture may be delayed because of

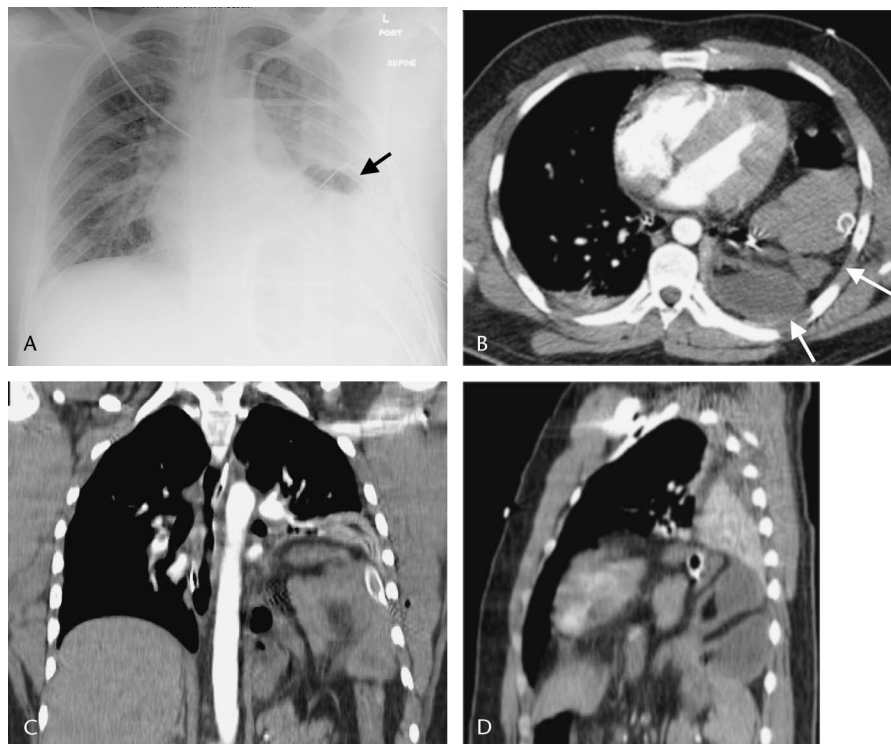


**FIGURE 8.** A, Supine chest radiograph of a 22-year-old man with diaphragmatic rupture from a car crash shows obliteration of the left hemidiaphragmatic outline, gas containing lesion in the left hemithorax (arrow), and mild deviation of the mediastinum to the contralateral side. B, Image from a multidetector CT scan of the chest shows abdominal organ abutting the posterior ribs (arrows), the dependent viscera sign. C, D, Coronal and sagittal reformations clearly demonstrate upward herniation of the abdominal organs into the left hemithorax.

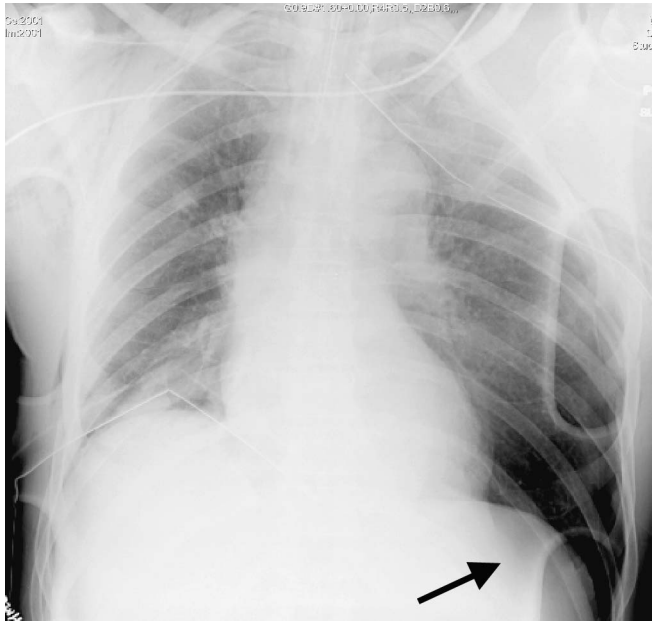


**FIGURE 9.** Supine chest radiograph of a 60-year-old man who fell down 10 stairs shows fractures of the left third through the ninth ribs, representing flail chest deformity. The deep sulcus sign on the left (arrow) reflects the underlying pneumothorax.

its rarity and its often non-specific clinical and radiographic manifestations.

The most common radiographic manifestations of tracheobronchial laceration are pneumomediastinum and pneumothorax, occurring in approximately 70% of patients.<sup>20</sup> The “fallen lung” sign, while diagnostic, rarely occurs, and represents complete disruption of all anchoring attachment of the lung to the hilum. The transected lung falls against the posterolateral chest wall or hemidiaphragm,<sup>21–23</sup> and there is a very dramatic hydropneumothorax.<sup>24</sup>

CT of the chest with an appropriate window setting can frequently show the exact site of tear, manifesting as a focal defect in or circumferential absence of the tracheal or bronchial wall, a central airway wall contour deformity (Fig. 6), abnormal communication of the central airway with other mediastinal structures,<sup>25–28</sup> over-distention of the endotracheal tube balloon (Fig. 7), herniation of the deformed endotracheal balloon beyond the trachea, or extraluminal location of the endotracheal tube.<sup>29</sup> Indirect signs, such as deep cervical emphysema and pneumomediastinum, should raise suspicion for tracheobronchial injury in the appropriate clinical setting.<sup>19,30–32</sup>

### Diaphragmatic Injury

Diaphragmatic injury occurs in up to 8% of patients suffering blunt trauma,<sup>33</sup> occurring most often in young men injured in motor vehicle crashes.<sup>34,35</sup>

Chest radiographic findings specific for diaphragmatic rupture include intrathoracic herniation of a hollow viscus and visualization of the nasogastric tube above the left hemidiaphragm (Fig. 8).<sup>33</sup> Other radiographic findings that are suggestive of but not specific for diaphragmatic injury include elevation of the hemidiaphragm, distortion or obliteration of the diaphragmatic outline, and contralateral shift of the mediastinum.<sup>36</sup> Even though chest radiographs are recommended in all patients suffering major trauma, they are insensitive for identifying diaphragmatic rupture (sensitivity of 46% for the left and 17% for the right).<sup>36</sup> Delayed rupture of the diaphragm has been reported in intubated patients, occurring when positive pressure ventilation is withdrawn.<sup>37</sup>

With the advent of helical and now MDCT technology, the diagnostic accuracy of CT for diaphragmatic injury has improved.<sup>38</sup> CT has reported sensitivity and specificity of 61–71% and 87–100%, respectively, for acute traumatic diaphragmatic rupture.<sup>39,40</sup> CT findings suggestive of hemidiaphragmatic rupture include discontinuity of the hemidiaphragm (73% sensitivity and 90% specificity),<sup>40,41</sup>

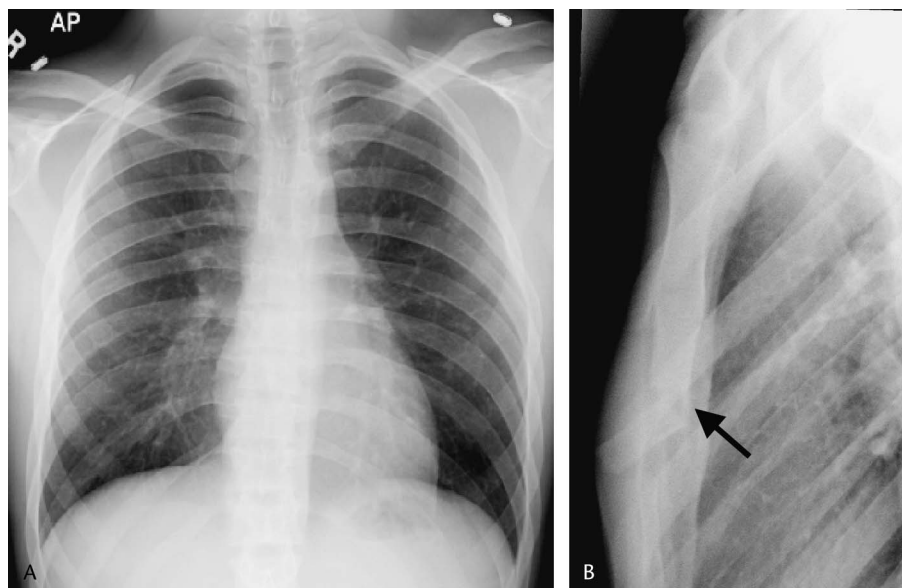


**FIGURE 10.** A, Supine chest radiograph of a 20-year-old man who complained of sternal tenderness after being involved in a high speed motor vehicle crash shows no abnormality. B, The coned down lateral view shows a displaced fracture of the sternal body (arrow).

intrathoracic herniation of abdominal contents (55% sensitivity and 100% specificity),<sup>40</sup> the collar sign (a waist-like constriction of the herniated hollow viscus at the site of the diaphragmatic tear with 63% sensitivity and 100% specificity),<sup>39</sup> and the dependent viscera sign (herniated viscera layering dependently in the hemithorax against the posterior ribs). One series reported a positive dependent viscera sign with 100% of left and 83% of right diaphragmatic injuries.<sup>34</sup>

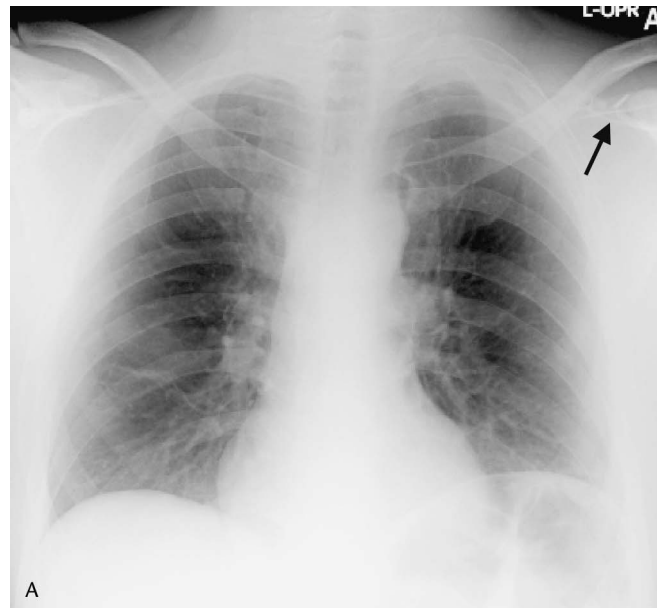


**FIGURE 11.** A, Supine chest radiograph of 25-year-old man who was involved in a motor vehicle crash shows fracture of the left scapular spine with displacement of a bony fragment (arrow). B, Fractures of the scapular body (double arrows) and scapular spine (arrows) are well demonstrated on the 3D-rendered image from the CT scan.

## CHEST WALL INJURY

### Rib Fractures

Rib fractures are the most common injury following blunt chest trauma.<sup>42,43</sup> The most common site of rib fractures are the lateral aspect of ribs 4–9 where there is less overlying musculature.<sup>15,44</sup> However, fracture of the first and/or second rib is a marker of high energy trauma since these ribs are short, thick, and relatively well-protected by the thoracic muscles.<sup>44</sup> Injuries associated with first and second rib fractures include pulmonary and cardiac contusion, neck injuries, and severe abdominal injuries.<sup>44,45</sup> Isolated first rib fractures are also associated with whiplash injuries.<sup>46</sup> Lacerations of the liver, spleen, and kidney are associated with fractures of ribs 9–12.<sup>44</sup>

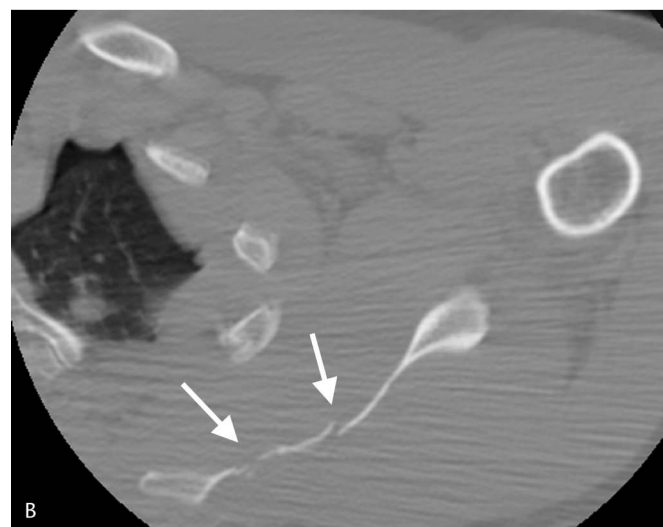


**FIGURE 12.** A, Supine chest radiograph of a 19-year-old man who was involved in a snow-boarding accident shows subcutaneous emphysema in the soft tissues of the left chest wall without evidence of scapular fracture. B, CT scan. The scapular fracture (arrows) is well demonstrated with multiplanar reformatted CT images.

While a common injury, not all rib fractures are identified on the initial chest radiograph, particularly when they are not displaced.<sup>47</sup> CT has proven to be useful in the setting of rib fractures not only because it can show non-displaced fractures, but also it can help identify injuries associated with rib fractures, such as pulmonary laceration or abdominal visceral injuries.

Flail chest deformity is a serious manifestation of rib fracture and is defined as 5 or more adjacent rib fractures or more than 3 segmental rib fractures.<sup>2,14,43,48</sup> Flail chest deformity can lead to respiratory failure from the direct effect of lung and pleural injury as well as impaired ventilation due to dysfunction of normal chest wall mechanics (Fig. 9).

### Sternal Fracture

Sternal fracture occurs in about 8% of patients admitted for blunt chest injury,<sup>49</sup> and the majority occur in elderly patients. Motor vehicle crashes are the cause of about 80% of sternal fractures.<sup>11</sup> Sternal fracture is generally a marker for high energy trauma and is associated with injuries to mediastinal structures including the heart, great vessels, and tracheobronchial tree.

Sternal fractures cannot be seen on a frontal chest radiograph. A lateral view may help identify a sternal fracture (Fig. 10), but CT is the examination of choice, especially because it can show associated mediastinal injuries.<sup>42</sup>

### Scapular Fracture

The scapula is a well-protected structure, and, therefore, a scapular fracture is a marker of high energy trauma. On the chest radiograph, scapular fracture is typically overlooked in up to 43% of patients. Moreover, 72% of these unobserved fractures are visible in retrospect on the initial radiograph.<sup>50</sup>

CT is more sensitive than radiography for detecting the fracture site and its associated injuries, which include rib fractures, pneumothorax, hemothorax, and pulmonary contusion (Figs. 11 and 12).<sup>42</sup>

### Thoracic Spine Fracture

Fracture of the thoracic spine accounts for approximately 25–30% of all spine fractures.<sup>51</sup> It usually occurs with motor vehicle crashes or with fall from great height. Thoracic spine fractures or dislocations have the highest incidence of associated neurologic deficits as compared to fractures elsewhere in the spine.<sup>35</sup>

The chest radiograph is not an adequate study to completely evaluate the thoracic spine. Dedicated frontal and lateral radiographs centered on and collimated to the thoracic spine are necessary to provide the minimally acceptable radiologic evaluation. Radiographic signs of thoracic spine fracture include cortical disruption, vertebral body height loss or deformity, abnormal vertebral alignment, focal mediastinal contour abnormality, and focal lateral displacement of the paravertebral stripe from paraspinal hematoma.<sup>1,52</sup>

CT is the modality of choice for evaluating spinal fracture because of its high sensitivity and the ability to reformat images in multiple planes, particularly with MDCT (Fig. 13).<sup>53</sup>

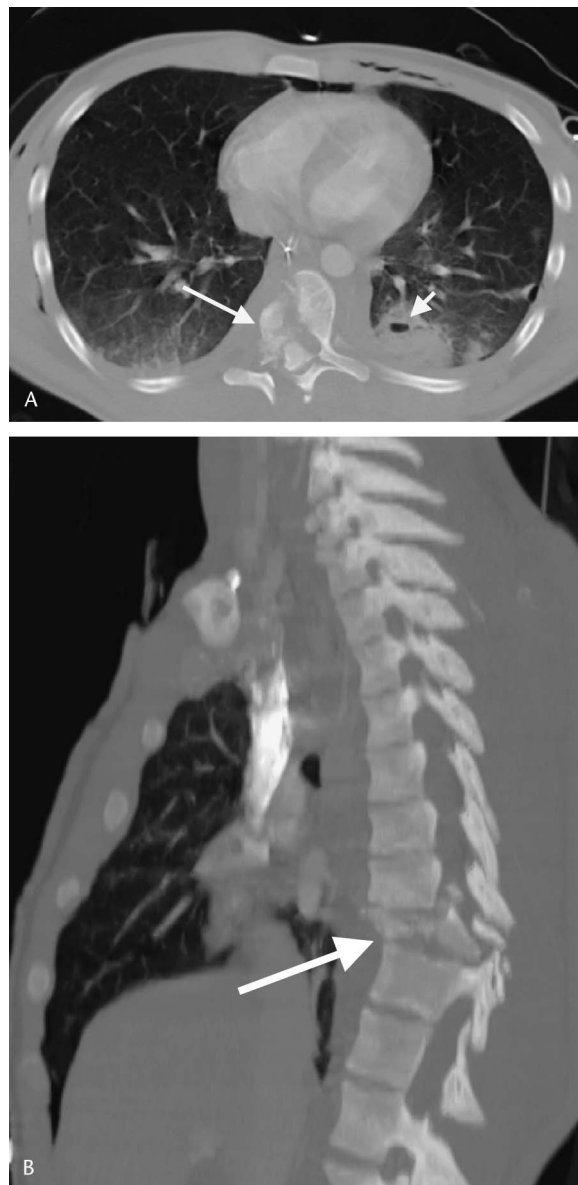


**FIGURE 13.** A, CT scan of the chest of a 19-year-old male who was injured from skiing shows comminuted fracture of the thoracic spine (long arrow) surrounded with paraspinal hematoma. A type 2 pulmonary laceration (short arrow) and pulmonary opacity abutting a right posterior rib (likely pulmonary contusion or aspiration) are also present. B, Sagittal reformation better delineates the severity of the fracture (arrow).

MRI is a useful adjunct imaging modality to evaluate spinal soft tissues, including the intervertebral discs, spinal ligaments, paravertebral soft tissues, spinal cord, and nerve roots, and also early detection of the bone marrow contusion or so called “bone bruise,” which is radiographically occult. However, MRI does not demonstrate actual fractures as well as do conventional radiography or CT,<sup>54–56</sup> and due to imaging time and difficulty with life support equipment, MRI is not generally used in the primary imaging evaluation.



**FIGURE 14.** A, Supine chest radiograph of a 36-year-old woman who was injured in a high speed motor vehicle crash shows abnormal contour of the mediastinum, haziness of the left hemithorax, and rightward deviation of the trachea. B, Image from a CT scan of the chest shows an incomplete, low attenuation linear band in the aortic lumen (arrow), consistent with aortic injury. C, 3D shaded surface display reconstruction from the same CT better shows the aortic pseudoaneurysm (arrows).

### TRAUMATIC AORTIC INJURY

Thoracic aortic injury (TAI) (Fig. 14) is one of the most life threatening injuries and usually occurs in the setting of high energy trauma to the chest and abdomen.<sup>1</sup> Clinical indicators of TAI are not reliable, and the diagnosis almost exclusively depends upon imaging.

The chest radiograph is a good screening examination, but remains a poor diagnostic tool as it has high sensitivity but low specificity. The following signs are suggestive of mediastinal hematoma, and, therefore, further imaging is warranted to evaluate for possible aortic rupture:

1. Abnormal mediastinal contour.
2. Blurring of aortic arch contour and opacity in the aortopulmonary window.<sup>57</sup>
3. A left apical pleural cap, and possibly a left pleural effusion.<sup>57</sup>
4. Deviation of the trachea or enteric tube to the right and displacement of the right paratracheal stripe and paraspinous line.<sup>58–60</sup>
5. Widening of the right paratracheal stripe more than 5 mm.<sup>61</sup>

While no single finding is diagnostic, the negative predictive value of a normal frontal chest radiograph for TAI is 98%.<sup>62</sup>

Catheter aortography has a very high sensitivity and specificity for TAI. Traditionally, it followed radiography in investigating TAI. The development of MDCT has improved the ability to image the thoracic aorta non-invasively and has led to CT becoming the primary imaging modality for TAI at many institutions following chest radiography.<sup>62,63</sup>

In addition to evaluating the thoracic aorta, CT aortography has the ability to image other structures, such as the lungs, pleura, heart, and chest wall.

CT findings of TAI are classified into direct and indirect signs.<sup>64</sup> Direct signs include pseudoaneurysm (most common), abnormal aortic contours or abrupt caliber change, pseudo-coarctation, occlusion of a segment of aorta, and intimal flap. Mediastinal and retrocrural hematoma are considered indirect signs. Hematomas that obliterate fat planes surrounding the otherwise normal appearing aorta or other great vessels are suggestive of occult injury and may need further investigation

with catheter aortography. In contrast, mediastinal hematoma that does not directly contact the aorta or great vessels usually represents mediastinal venous bleeding, and aortography is not generally indicated.<sup>64</sup>

One study by Gavant and coworker showed that helical CT has 100% sensitivity and at least 83% specificity for detecting TAI.<sup>65</sup> Although results regarding the use of MDCT for evaluating TAI are not yet available, they are expected to be equal to or better than those obtained with single slice helical CT.

### CONCLUSION

Chest imaging plays an important role in the diagnosis of blunt chest trauma, as the history and physical examination are often unreliable. However, the radiologist should be aware of the limitations of the supine chest radiograph to minimize “over” or “under” interpretation. CT has become a central imaging modality used to evaluate patients suffering from blunt injury to the chest, and MDCT has allowed for better spatial resolution and decreased scan time.

### REFERENCES

1. Groskin SA. Selected topics in chest trauma. *Radiology*. 1992;183:605–617.
2. Greene R. Blunt thoracic trauma. In: *Syllabus: a Categorical Course in Diagnosis Radiology: Chest Radiology*. Oak Brook, IL: Radiological Society of North America; 1992:297–309.
3. Besson A, Saegesser FA. Lung injury from blunt chest trauma. In: *Color Atlas of Chest Trauma and Associated Injuries*. Weert, Netherlands: Wolfe; 1982:156–166.
4. Rivas LA, Fishman JE, Munera F, et al. Multislice CT in thoracic trauma. *Radiol Clin North Am*. 2003;41:599–616.
5. Greenberg MD, Rosen CL. Evaluation of the patient with blunt chest trauma: an evidence based approach. *Emerg Med Clin North Am*. 1999; 17:41–62.
6. Keough V, Pudelek B. Blunt chest trauma: review of selected pulmonary injuries focusing on pulmonary contusion. *AACN Clin Issues*. 2001;12: 270–281.
7. Wagner RB, Crawford WO Jr, Schimpf PP. Classification of parenchymal injuries of the lung. *Radiology*. 1988;167:77–82.

8. Dee P. Chest trauma. In: Armstrong P, Wilson AG, Dee P, et al, eds. *Imaging of Diseases of the Chest*. London: Mosby; 2000:949–981.
9. Ashbaugh DG, Peters GN, Halgrimson CG, et al. Chest trauma. Analysis of 685 patients. *Arch Surg*. 1967;95:546–555.
10. Conn JH, Hardy JD, Fain WR, et al. Thoracic trauma: analysis of 1022 cases. *J Trauma*. 1963;3:22–40.
11. Chan O, Hiorns M. Chest trauma. *Eur J Radiol*. 1996;23:23–34.
12. Ziter FM Jr, Westcott JL. Supine subpulmonary pneumothorax. *AJR Am J Roentgenol*. 1981;137:699–701.
13. Dee PM. The radiology of chest trauma. *Radiol Clin North Am*. 1992;30:291–306.
14. Kazerooni EA, Gross BH. Thoracic trauma. In: Kazerooni EA, Gross BH, eds. *Core Curriculum: Cardiopulmonary Imaging*. Philadelphia, PA: Lippincott Williams & Wilkins Publishers; 2004:295–322.
15. Richardson JD, Spain DA. Injury to the lung and pleura. In: Mattox KL, Feliciano DV, Moore EA, eds. *Trauma*. New York: McGraw-Hill Publishers; 2000:523–543.
16. Bowling WM, Wilson RF, Kelen GD, et al. Thoracic trauma. In: Tintinalli JE, Kelen GD, Stapczynski JS, eds. *Emergency Medicine*. New York: McGraw-Hill; 2000:251.
17. Bertelsen S, Howitz P. Injuries of the trachea and bronchi. *Thorax*. 1972;27:188–194.
18. Wiot JF. Tracheobronchial trauma. *Semin Roentgenol*. 1983;18:15–22.
19. Kirsh MM, Orringer MB, Behrendt DM, et al. Management of tracheobronchial disruption secondary to nonpenetrating trauma. *Ann Thorac Surg*. 1976;22:93–101.
20. Ketai L, Brandt MM, Schermer C. Nonaortic mediastinal injuries from blunt chest trauma. *J Thorac Imaging*. 2000;15:120–127.
21. Oh KS, Fleischner FG, Wyman SM. Characteristic pulmonary finding in traumatic complete transection of a main-stem bronchus. *Radiology*. 1969;92:371–372.
22. Kumpe DA, Oh KS, Wyman SM. A characteristic pulmonary finding in unilateral complete bronchial transection. *Am J Roentgenol Radium Ther Nucl Med*. 1970;110:704–706.
23. Petterson C, Deslauriers J, McClish A. A classic image of complete right main bronchus avulsion. *Chest*. 1989;96:1415–1417.
24. Unger JM, Schuchmann GG, Grossman JE, et al. Tears of the trachea and main bronchi caused by blunt trauma: radiologic findings. *AJR Am J Roentgenol*. 1989;153:1175–1180.
25. Lupetin AR. Computed tomographic evaluation of laryngotracheal trauma. *Curr Probl Diagn Radiol*. 1997;26:185–206.
26. Palder SB, Shandling B, Manson D. Rupture of the thoracic trachea following blunt trauma: diagnosis by CAT scan. *J Pediatr Surg*. 1991;26:1320–1322.
27. d'Odemont JP, Pringot J, Goncette L, et al. Spontaneous favorable outcome of tracheal laceration. *Chest*. 1991;99:1290–1292.
28. Baumgartner FJ, Ayres B, Theuer C. Danger of false intubation after traumatic tracheal transection. *Ann Thorac Surg*. 1997;63:227–228.
29. Chen JD, Shanmuganathan K, Mirvis SE, et al. Using CT to diagnose tracheal rupture. *AJR Am J Roentgenol*. 2001;176:1273–1280.
30. Eijgelaar A, Homan van der Heide JN. A reliable early symptom of bronchial or tracheal rupture. *Thorax*. 1970;25:120–125.
31. Spencer JA, Rogers CE, Westaby S. Clinico-radiological correlates in rupture of the major airways. *Clin Radiol*. 1991;43:371–376.
32. Lotz PR, Martel W, Rohwedder JJ, et al. Significance of pneumomediastinum in blunt trauma to the thorax. *AJR Am J Roentgenol*. 1979;132:817–819.
33. Iochum S, Ludig T, Walter F, et al. Imaging of diaphragmatic injury: a diagnostic challenge? *Radiographics*. 2002;22 Spec No:S103–S116.
34. Bergin D, Ennis R, Keogh C, et al. The “dependent viscera” sign in CT diagnosis of blunt traumatic diaphragmatic rupture. *AJR Am J Roentgenol*. 2001;177:1137–1140.
35. Van Hise ML, Primack SL, Israel RS, et al. CT in blunt chest trauma: indications and limitations. *Radiographics*. 1998;18:1071–1084.
36. Gelman R, Mirvis SE, Gens D. Diaphragmatic rupture due to blunt trauma: sensitivity of plain chest radiographs. *AJR Am J Roentgenol*. 1991;156:51–57.
37. Carter YM, Karmy-Jones RC, Stern EJ. Delayed recognition of diaphragmatic rupture in a patient receiving mechanical ventilation. *AJR Am J Roentgenol*. 2001;176:428.
38. Blum A, Walter F, Ludig T, et al. Multislice CT: principles and new CT-scan applications. *J Radiol*. 2000;81:1597–1614.
39. Killeen KL, Mirvis SE, Shanmuganathan K. Helical CT of diaphragmatic rupture caused by blunt trauma. *AJR Am J Roentgenol*. 1999;173:1611–1616.
40. Murray JG, Caoili E, Gruden JF, et al. Acute rupture of the diaphragm due to blunt trauma: diagnostic sensitivity and specificity of CT. *AJR Am J Roentgenol*. 1996;166:1035–1039.
41. Worthy SA, Kang EY, Hartman TE, et al. Diaphragmatic rupture: CT findings in 11 patients. *Radiology*. 1995;194:885–888.
42. Kerns SR, Gay SB. CT of blunt chest trauma. *AJR Am J Roentgenol*. 1990;154:55–60.
43. Kuhlman JE, Pozniak MA, Collins J, et al. Radiographic and CT findings of blunt chest trauma: aortic injuries and looking beyond them. *Radiographics*. 1998;18:1085–1106; discussion 1107–1108; quiz 1. Review.
44. Cogbill TH, Landercasper J. Injury to the chest wall. In: Mattox KL, Feliciano DV, Moore EE, eds. *Trauma*. New York: McGraw-Hill; 2000:483–504.
45. Miller FB, Richardson JD, Thomas HA, et al. Role of CT in diagnosis of major arterial injury after blunt thoracic trauma. *Surgery*. 1989;106:596–602.
46. Qureshi T, Mander BJ, Wishart GC. Isolated bilateral first rib fractures—an unusual sequel of whiplash injury. *Injury*. 1998;29:397–398.
47. Tocino I, Miller MH. Computed tomography in blunt chest trauma. *J Thorac Imaging*. 1987;2:45–59.
48. Gurney JW. ABCs of blunt chest trauma. In: *Thoracic imaging*. Reston, VA: Society of Thoracic Radiology; 1996:349–352.
49. Fisher RG, Ward RE, Ben-Menachem Y, et al. Arteriography and the fractured first rib: too much for too little? *AJR Am J Roentgenol*. 1982;138:1059–1062.
50. Harris RD, Harris JH Jr. The prevalence and significance of missed scapular fractures in blunt chest trauma. *AJR Am J Roentgenol*. 1988;151:747–750.
51. Pal JM, Mulder DS, Brown RA, et al. Assessing multiple trauma: is the cervical spine enough? *J Trauma*. 1988;28:1282–1284.
52. Daffner RH. *Imaging of Vertebral Trauma*. Rockville, IL: Aspen; 1988.
53. el-Khoury GY, Whitten CG. Trauma to the upper thoracic spine: anatomy, biomechanics, and unique imaging features. *AJR Am J Roentgenol*. 1993;160:95–102.
54. Goldberg AL, Rothfus WE, Deeb ZL, et al. The impact of magnetic resonance on the diagnostic evaluation of acute cervicothoracic spinal trauma. *Skeletal Radiol*. 1988;17:89–95.
55. Kalfas I, Wilberger J, Goldberg A, et al. Magnetic resonance imaging in acute spinal cord trauma. *Neurosurgery*. 1988;23:295–299.
56. Mathis JM, Wilson JT, Barnard JW, et al. MR imaging of spinal cord avulsion. *AJNR Am J Neuroradiol*. 1988;9:1232–1233.
57. Simeone JF, Deren MM, Cagle F. The value of the left apical cap in the diagnosis of aortic rupture: a prospective and retrospective study. *Radiology*. 1981;139:35–37.
58. Gerlock AJ Jr, Muhletaler CA, Coulam CM, et al. Traumatic aortic aneurysm: validity of esophageal tube displacement sign. *AJR Am J Roentgenol*. 1980;135:713–718.
59. Marnocha KE, Maglinte DD. Plain-film criteria for excluding aortic rupture in blunt chest trauma. *AJR Am J Roentgenol*. 1985;144:19–21.
60. Tisnado J, Tsai FY, Als A, et al. A new radiographic sign of acute traumatic rupture of the thoracic aorta: displacement of the nasogastric tube to the right. *Radiology*. 1977;125:603–608.
61. Peters DR, Gamsu G. Displacement of the right paraspinous interface: a radiographic sign of acute traumatic rupture of the thoracic aorta. *Radiology*. 1980;134:599–603.
62. Mirvis SE, Bidwell JK, Buddemeyer EU, et al. Value of chest radiography in excluding traumatic aortic rupture. *Radiology*. 1987;163:487–493.
63. Gundry SR, Williams S, Burney RE, et al. Indications for aortography in blunt thoracic trauma: a reassessment. *J Trauma*. 1982;22:664–671.
64. Gotway MB, Dawn SK. Thoracic aorta imaging with multislice CT. *Radiol Clin North Am*. 2003;41:521–543.
65. Gavant ML, Menke PG, Fabian T, et al. Blunt traumatic aortic rupture: detection with helical CT of the chest. *Radiology*. 1995;197:125–133.